*Eco. Env. & Cons. 28 (3) : 2022; pp. (1473-1477)*
*Copyright@ EM International*
*ISSN 0971–765X*

**DOI No.: http://doi.org/10.53550/EEC.2022.v28i03.052**

# Biocompatible Herbal Polymeric Nano-formulation of [6]-Gingerol: Development, Optimisation, and Characterization

**Virendra Singh[1]*, Himanshu Pandey[1], Vatsala Misra[2] and Devendra Singh[3]**

***[1]Department of Pharmaceutical Sciences, Sam Higginbottom University of Agriculture (SHUATS), Prayagraj, India***
***[2]Department of Pathology, Motilal Nehru Medical College, Prayagraj, India***
***[3]Department of Biotechnology, B.N. College of Engineering and Technology, Lucknow, India***

(Received 22 October, 2021; Accepted 13 December, 2021)

**ABSTRACT**

Ginger has a long reported history as a spice, and India is the largest cultivator of ginger in the world. The study was aimed to develop sustained release herbal polymeric nano-formulation with [6]-Gingerol for anti-microbial activity without any adverse effect on the environment. [6]-Gingerol-loaded polymeric nanoparticles were developed by the single emulsification solvent evaporation method. 4%w/v Polyvinyl alcohol (PVA) was used as an aqueous phase, while [6]-Gingerol and Eudragit in acetone were used as an organic phase. The Box-Behnkendesign (BBD) was used to determine the effect of independent variables on responses. The particle size, zeta potential, and % entrapment efficiency were recorded as 319± 3.32 nm, +26±1.11 mV, and 78±0.89, respectively.

***Key words :*** *Ginger,[6]-Gingerol, Box-Behnken design, Polymeric nanoformulation.*

## Introduction

Ginger has been used as herbal medicine since ancient times (Shahrajabian *et al.,* 2019). A tropical and subtropical climate with 19-28°C is favorable for the cultivation of ginger. It has wider adaptability for a different type of soil, but for maximum production, the soil should be loose, friable, and offer maximum resistance to rhizome development (Kandiannan *et al.,* 1996). The optimum time for harvesting ginger in India is about 7-9 months days after planting (Bag, 2018). Conservation of ginger germplasm is done by *in-vitro* preservation and cryopreservation. The *in-vitro* preservation method has a complementary approach to genotype conservation, while cryopreservation is the long-term conservation of germplasm (Yamuna *et al.,* 2007).

The ginger rhizome and its extract have also been extensively used as a traditional medicine to treat cough, cold, vomiting, indigestion, rheumatism, infectious disease, and many other diseases (Wei *et al.,* 2018). [6]-Gingerol is the most abundant bioactive polyphenolic compound of *Zingiber officinale* (Manatunga *et al.,* 2018). [6]-Gingerol is a potent antimicrobial (Chiaramonte *et al.,* 2021), anti-inflammatory (Faria *et al.,* 2021), and hypolipidemic constituent of ginger (Shao *et al.,* 2016). Polymeric nanoparticles as drug carriers are widely used for controlled release drug delivery systems. They can protect drugs and other molecules from biological activity against the environment and improve their bioavailability and therapeutic index (Owens and

Peppas, 2006). Polymeric carriers are biocompatible, non-toxic, non-immunogenic, biodegradable, inexpensive, and easy to synthesize (Bolhassani *et al.*, 2014).

In this study, we developed [6]-Gingerol-loaded polymeric nanoparticles by using a single emulsification solvent evaporation method. The obtained product was centrifuged, lyophilized, and stored in an airtight vial for the characterization process.

## Materials and Methods

The primary raw materials used for the study included [6]-Gingerol purchased from Shaanxi Pioneer Biotech Co. Ltd., and the rest of the chemicals were bought from Fisher Scientific, Mumbai, India. Water for injection (WFI), used as a vehicle throughout the formulation procedure.

### Formulation and Development

The single emulsification solvent evaporation method was used for the development of [6]-Gingerol-loaded Eudragit nanoparticles (Vardhan*et al.*, 2017). The organic phase was prepared by dissolving [6]-Gingerol (1mg) and Eudragit (4.46 mg) in acetone. 4%w/v Polyvinyl alcohol (PVA) was used as an aqueous phase. The organic phase was added into the aqueous phase and stirred continuously to form a uniform mixture. The mixture was homogenized via IKA high shear homogenizer at 15000 rpm for 10 minutes and sonicated using Ultra Probe sonicator (UP50H, Hielscher) for 15 minutes. The formulation was then stirred on the magnetic stirrer (IKARH digital) at the speed of 500 rpm and left overnight for the evaporation of the organic solvent. The obtained product was centrifuged, lyophilized, and stored in an air-tight vial for physical and chemical characterization process and further use.

### Optimization

The [6]-Gingerol-loaded polymeric nanoparticles were optimized by Box-Behnken design (BBD) using Minitab 7 software. The levels of independent variables (factors) were determined by pre-formulation screening and data computation methods. After the factors were screened, the independent variables, [A] polymer concentration (mg), [B] surfactant concentration (mg), [C] homogeniser speed (rpm) and [D] ultra-sonication time (min) were optimized. The factorial design was chosen to generate the quadratic equation that explains the effect of independent variables. By the application of both experimental and factorial design, the predicted formulation was optimized, which was used further for in-vitro characterization.

### Characterization

### Determination of particle size and charge

The particle size was determined by using a Zeta sizer (Inkson, 2016). The surface charge was determined by a dynamic scattering analyzer (Desla Nano C, Beckman Coulter, UK) in a polystyrene cuvette that determines the stability of the product. The electrophoretic mobility (electric field strength and viscosity), physical stability, and colloidal property of the formulation were measured by Zeta potential.

### Entrapment Efficiency

The entrapment efficiency was determined by applying the centrifugation method by separation of the supernatant free drug content (Fazil *et al.*, 2012). A known quantity of [6]-Gingerol nanoparticles is suspended in acetone and subjected to centrifugation at 10,000 rpm for 10 min. The supernatant-free drug was analyzed using a UV-visible spectrophotometer at the wavelength of 430nm.

$$\%EE = \left(\frac{\text{Drug incorporated} - \text{free drug}}{\text{Drug incorporated}}\right) \times 100$$

### Drug-Polymer interaction

Fourier Transform Infrared Spectroscopy (FTIR, SHIMADZU 8400, Japan) was done to assess the compatibility of [6]-Gingerol with excipients (Mukherjee *et al.*, 2005). The sample was prepared with potassium bromide in a 100:1 ratio and scanned from the range of 4000 to 400 $cm^{-1}$ wavenumbers at room temperature.

## Results and Discussion

### Experimental Design: Box-Behnken

Box-Behnken Design (BBD) was used with 4 factors, 3 levels, and 3 center points (Table 1). The quadratic response surface technique generates 27 runs. The significant factors were identified by application of analysis of variance (ANOVA) at a 95% confidence interval. The effect of independent variables on par-

**Table 1.** Levels of Independent and Dependent variables in Box-Behnken design

| Independent Variables (Factors) | | Levels | | |
|---|---|---|---|---|
| | | Low (-1) | Medium (0) | High (+1) |
| A | Polymer concentration | 1 | 4.5 | 8 |
| B | Surfactant concentration | 1 | 2.5 | 4 |
| C | Homogeniser Speed (rpm) | 15000 | 17500 | 20000 |
| D | Ultra-Sonication Time (min) | 10 | 12.5 | 15 |
| Dependent variables (response) | | Constraint | | |
| R1 | Particle Size | 150-450 | | |
| R2 | Zeta Potential (mV) | Maximum | | |
| R3 | Entrapment Efficiency (%) | Maximum | | |

ticle size, entrapment efficiency, and zeta potential is determined by Minitab 7 software (Fig.1). The Surface plot (Fig. 2) was generated for the quantification of correlation and interaction between the independent variables and obtained response (Beg *et al.*, 2013; Cao *et al.*, 2013). The optimized values of independent variables predicted the results of dependent variables, and the experimental findings of particle size (nm), zeta potential (mV), and entrapment efficiency (%) are shown in Table 2. The predicted values showed satisfactory correlation and minimum bias with experimental findings. The optimized formulation was selected for further studies.

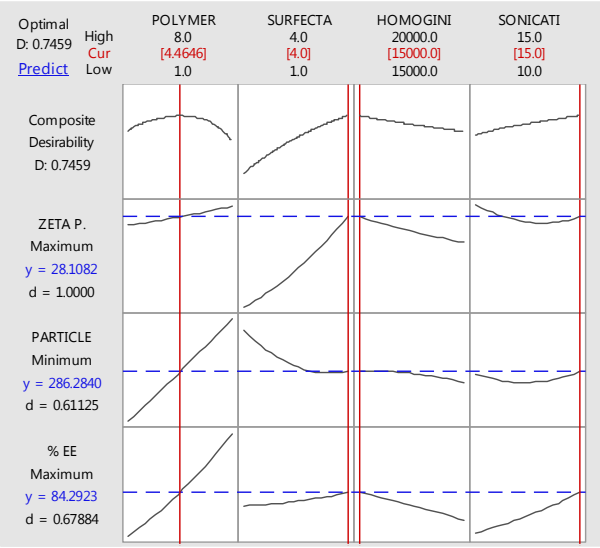


**Fig. 1.** Optimized anticipated setpoints of independent variables showing the effects on particle size, zeta potential and entrapment efficiency.

The particle size is a decisive factor for nanoparticle-based drug delivery systems. The biodistribution pattern kinetics of drug release and stability of nanoparticles depends on the particle size (Son *et al.*, 2017). The quadratic model has a p-value <0.05 and F- value 06.01 representing the best fit for particle size. The regression coefficient of 86.66 % indicates a good relationship between the estimated and obtained values. The lack of fit for the particle was 0.66, which indicated a good fit (p>0.05) in the model (Table 3). Hence the model is suitable to optimize the formulation. The polymer concentration plays a significant role in the determination of particle size. The ultrasonication time is inversely proportional to the particle size that causes an increase in the shear stress. The high shear stress leads to the formation of smaller particles. The predicted particle size was 86.28 nm, while the experimental

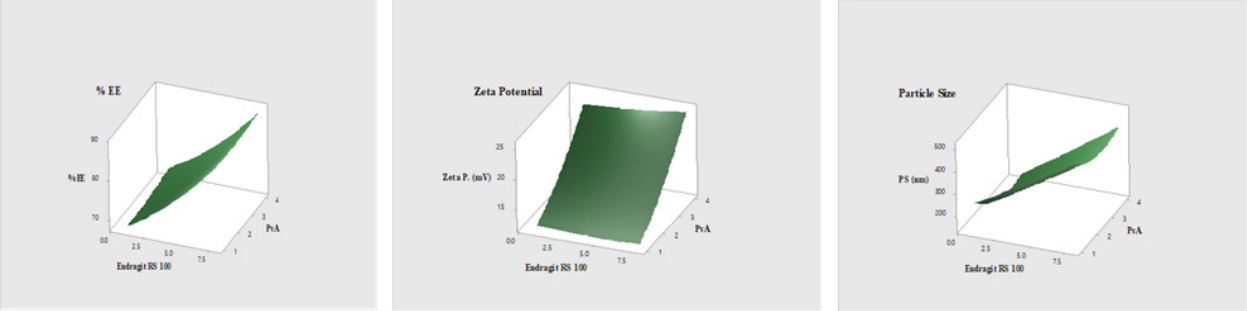


**Fig. 2.** 3-D Response Surface graph showing the effect of independent variables on Responses: % Entrapment efficiency (A), Zeta potential (B) and Particle size (C). Effect of independent variables on particle size

**Table 2.** The optimized value of Independent Variables using BBD

| Independent Variables | | | |
|---|---|---|---|
| A | Polymer (mg) | 4.46 | |
| B | Surfactant (mg) | 4 | |
| C | Homogeniser Speed (rpm) | 15000 | |
| D | Ultra-Sonication Time (min) | 15 | |
| Optimised Result | | | |
| Dependent variable (response) | | Predicted Value | Experimental Value* |
| R1 | Particle Size | 286.28 | 319± 3.32 |
| R2 | Zeta Potential (mV) | +28.11 | +26±1.11 |
| R3 | Entrapment Efficiency (%) | 84.29 | 78±0.89 |

* Value expressed in Mean ± SEM (n=3)

**Table 3.** Statistical Analysis of Linear model

| Response | Linear model | | | | |
|---|---|---|---|---|---|
| | F-Value | p-Value* | R-Sq (%) | Lack of fit | Remark |
| P. size | 06.01 | <0.05 | 86.66 | 0.66 | Significant |
| % EE | 17.16 | <0.05 | 91.93 | 0.78 | Significant |
| ZP (mV) | 07.28 | <0.05 | 89.71 | 0.174 | Significant |

mean particle size was 319± 3.32.

### Effect of independent variables on Zeta potential

The F-value obtained from the quadratic model was 07.28 and was marked as significant ($p<0.05$). The regression coefficient of the model was 89.71%, showing the best fit. The experimental model exhibited sufficient fit to data, and lack of fit was absent with a p-value of 0.174 ($p>0.05$) (Table 3). A significant increase in zeta potential was seen with an increase in the surfactant concentration due to the interfacial phenomenon. The predicted zeta potential was +28.11mV, while the experimental zeta potential was +26±1.11mV.

### Effect of independent variables on entrapment efficiency

The entrapment efficiency of the formulation varied from 76 % to 81 % due to a combination of various factors. The quadratic model was significant ($p<0.05$), having an F-value of 17.16. The lack of fit for entrapment efficiency was found to be 0.78 (Table 3). The regression coefficient was significant, indicating reasonable adequacy and fit the model. The predicted entrapment efficiency was 84.29%, while the experimental entrapment efficiency was found to be78±0.89.

### FTIR analysis

FTIR spectra (Fig. 3) of [6]-Gingerol powder showed a characteristic band at 1035 corresponding to the stretching of -CHOH of [6]-Gingerol. The widened band centered near 3400 cm-1 represents the presence of -OH stretching.

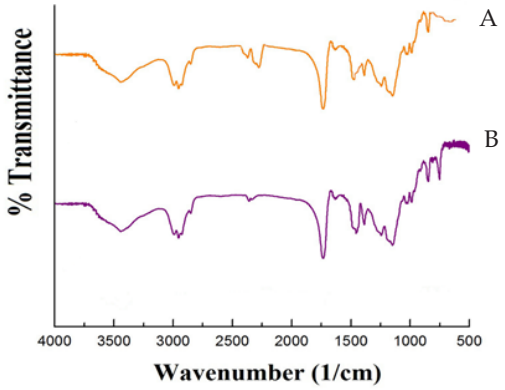


**Fig. 3.** FTIR spectra of A: [6]-Gingerol and B: Nanoformulation

The presence of [6]-Gingerol absorption bands in formulation assured no chemical reaction between the drug and excipients.

## Conclusion

The present study highlighted the prominence of the green approach in the formulation of nanoparticles

with the active ingredient of ginger rhizome. The herbal drug component gives an edge over the standard treatment therapies, with reduced adverse effects and acceptability among the masses. A further formulation will be developed to treat contaminated media, including water, soil, and subsurface material. Hence, we conclude that this study serves as a helpful reference for future researches, highlighting the importance of [6]-Gingerol-based formulations.

**Conflict of Interest**

The authors confirm that there is no conflict of interest.

## Acknowledgment

The authors express their gratitude to Prof. Avinash Chandra Pandey, Nano-Application Center (NAC) Allahabad University, for his continued guidance and support.

## References

Bag, B. B. 2018. Ginger processing in India (Zingiber officinale): A review. *Int J Curr Microbiol App Sci.* 7: 639-1651.

Beg, S., Jena, S. S., Patra, C. N., Rizwan, M., Swain, S., Sruti, J. and Singh, B. 2013. Development of solid self-nanoemulsifying granules (SSNEGs) of ondansetron hydrochloride with enhanced bioavailability potential. *Colloids Surf B Biointerfaces*. 101: 414-423.

Bolhassani, A., Javanzad, S., Saleh, T., Hashemi, M., Aghasadeghi, M. R. and Sadat, S. M. 2014. Polymeric nanoparticles: potent vectors for vaccine delivery targeting cancer and infectious diseases. *Hum Vaccin Immunother.* 10: 321-332.

Cao, L., Li, G., Yang, D., Liu, J. and Huang, Y. 2013. Application of Response Surface Methodology to Formulation Optimization of Rapamycin Loaded Magnetic $Fe_3O_4$/Carboxymethylchitosan Nanoparticles. *J. Macromol. Sci. A*. 50 : 894-904.

Chiaramonte, M., Bonaventura, R., Costa, C., Zito, F. and Russo, R. 2021. [6]-Gingerol dose-dependent toxicity, its role against lipopolysaccharide insult in sea urchin (*Paracentrotus lividus* Lamarck), and antimicrobial activity. *Food Biosci.* 39 : 100833.

Faria, T. R. B., Furletti-Goes, V. F., Franzini, C. M., de Aro, A. A., de Andrade, T. A. M., Sartoratto, A. and de Menezes, C. C. 2021. Anti-inflammatory and antimicrobial effects of *Zingiber officinale* mouthwash on patients with fixed orthodontic appliances. *Am J Orthod Dentofacial Orthop.* 159 : 21-29.

Fazil, M., Md, S., Haque, S., Kumar, M., Baboota, S., Sahni, J. K. and Ali, J. 2012. Development and evaluation of rivastigmine loaded chitosan nanoparticles for brain targeting. *Eur J Pharm Sci.* 47 : 6-15.

Inkson, B. J. 2016. 2 - Scanning electron microscopy (SEM) and transmission electron microscopy (TEM) for materials characterization. In G. Hübschen, I. Altpeter, R. Tschuncky & H.-G. Herrmann (Eds.), *Materials Characterization Using Nondestructive Evaluation (NDE) Methods*. 17-43.

Kandiannan, K., Sivaraman, K., Thankamani, C. and Peter, K. 1996. Agronomy of ginger (*Zingiber officinale* Rosc.). *J. Spices and Aromatic Crops.* 5 : 1-27.

Manatunga, D. C., de Silva, R. M., de Silva, K. M. N., Wijeratne, D. T., Malavige, G. N. and Williams, G. 2018. Fabrication of 6-gingerol, doxorubicin and alginate hydroxyapatite into a bio-compatible formulation: enhanced anti-proliferative effect on breast and liver cancer cells. *Chem. Cent. J.* 12: 119.

Mukherjee, B., Mahapatra, S., Gupta, R., Patra, B., Tiwari, A. and Arora, P. 2005. A comparison between povidone-ethylcellulose and povidone-eudragit transdermal dexamethasone matrix patches based on *in vitro* skin permeation. *Eur J Pharm Biopharm.* 59: 475-483.

Owens, D. E., and Peppas, N. A. 2006. Opsonization, biodistribution, and pharmacokinetics of polymeric nanoparticles. *Int J Pharm.* 307 : 93-102.

Shahrajabian, M. H., Sun, W. and Cheng, Q. 2019. Clinical aspects and health benefits of ginger (*Zingiber officinale*) in both traditional Chinese medicine and modern industry. *Acta Agric Scand B Soil Plant Sci.* 69 : 546-556.

Shao, Y., Yu, Y., Li, C., Yu, J., Zong, R. and Pei, C. 2016. Synergistic effect of quercetin and 6-gingerol treatment in streptozotocin induced type 2 diabetic rats and poloxamer P-407 induced hyperlipidemia. *RSC Adv.* 6 : 12235-12242.

Son, G. H., Lee, B. J. and Cho, C. W. 2017. Mechanisms of drug release from advanced drug formulations such as polymeric-based drug-delivery systems and lipid nanoparticles. *Int. J. Pharm. Investig.* 47 : 287-296.

Vardhan, H., Mittal, P., Adena, S. K. and Mishra, B. 2017. Long-circulating polyhydroxybutyrate-co-hydroxyvalerate nanoparticles for tumor targeted docetaxel delivery: Formulation, optimization and *in vitro* characterization. *Eur J Pharm Sci.* 99 : 85-94.

Wei, Q., Yang, Q., Wang, Q., Sun, C., Zhu, Y., Niu, Y. and Xu, X. 2018. Formulation, Characterization, and Pharmacokinetic Studies of 6-Gingerol Loaded Nanostructured Lipid Carriers. *AAPS Pharm Sci Tech.* 19 : 3661-3669.

Yamuna, G., Sumathi, V., Geetha, S., Praveen, K., Swapna, N. and Nirmal Babu, K. 2007. Cryopreservation of *in vitro* grown shoots of ginger (*Zingiber officinale* Rosc.). *Cryo Letters.* 28 : 241-252.